# The mouse homeobox gene *Noto* regulates node morphogenesis, notochordal ciliogenesis, and left–right patterning

**Anja Beckers*, Leonie Alten*, Christoph Viebahn†, Philipp Andre‡, and Achim Gossler*§**

*Institute for Molecular Biology, Medizinische Hochschule Hannover, Carl-Neuberg-Strasse 1, D-30625 Hannover, Germany; †Zentrum Anatomie, Universität Göttingen, Kreuzbergring 36, 37075 Göttingen, Germany; and ‡Institute of Zoology (220), University of Hohenheim, Garbenstrasse 30, D-70593 Stuttgart, Germany

Edited by Kathryn V. Anderson, Sloan–Kettering Institute, New York, NY, and approved August 13, 2007 (received for review May 9, 2007)

**The mouse homeobox gene *Noto* represents the homologue of zebrafish floating head (*flh*) and is expressed in the organizer node and in the nascent notochord. Previous analyses suggested that *Noto* is required exclusively for the formation of the caudal part of the notochord. Here, we show that *Noto* is also essential for node morphogenesis, controlling ciliogenesis in the posterior notochord, and the establishment of laterality, whereas organizer functions in anterior–posterior patterning are apparently not compromised. In mutant embryos, left–right asymmetry of internal organs and expression of laterality markers was randomized. Mutant posterior notochord regions were variable in size and shape, cilia were shortened with highly irregular axonemal microtubuli, and basal bodies were, in part, located abnormally deep in the cytoplasm. The transcription factor *Foxj1*, which regulates the dynein gene *Dnahc11* and is required for the correct anchoring of basal bodies in lung epithelial cells, was down-regulated in mutant nodes. Likewise, the transcription factor *Rfx3*, which regulates cilia growth, was not expressed in *Noto* mutants, and various other genes important for cilia function or assembly such as *Dnahc5* and *Nphp3* were down-regulated. Our results establish *Noto* as an essential regulator of node morphogenesis and ciliogenesis in the posterior notochord, and suggest *Noto* acts upstream of *Foxj1* and *Rfx3*.**

cilia | left–right asymmetry | posterior notochord

The organizer of vertebrate embryos is essential for the establishment of the body plan during gastrulation and induces and patterns surrounding tissues. The inducing properties of the organizer are regulated by a network of genes that are expressed in the organizer and its derivatives (1–4). The *Not* genes form a group of homeobox genes that are expressed in the organizer and notochord and function in specifying axial mesoderm in zebrafish and *Xenopus* embryos (5). During gastrulation, the mouse Not homeobox gene *Noto* (formerly called *Not*) is expressed in the anterior primitive streak/organizer and in the posterior extreme of the forming notochord [posterior notochord (PNC)] (6, 7), which at embryonic day (E)7.5 is referred to as the node, a shallow, crescent-shaped depression on the endodermal (ventral) side at the distal tip of the embryo (8). *Noto* acts downstream of the organizer genes *Foxa2* and *T* and a null allele-disrupted normal notochord formation in and posterior to the lumbar region (7).

The node/PNC that emerges during gastrulation (and equivalent structures in other vertebrate classes) is crucial for the establishment of left–right asymmetry. In mouse and rabbit embryos, each cell on the ventral side of the PNC, which has a plate like appearance until well after the first somites form, carries a single primary cilium on its surface (8, 9). These primary cilia are unique because they are motile, but their axonemes contain only the nine regular-spaced peripheral doublet microtubules and lack the central microtubule pair that is usually present in motile cilia (10, 11). Functional cilia in the PNC, and in the equivalent gastrocoel roof plate and Kupffer's vesicle of *Xenopus* and zebrafish embryos, respectively, are critical for generating molecular asymmetry (12–15). In the PNC, cilia rotate clockwise and generate a leftward nodal flow (15) that generates an asymmetric signal either by establishing a gradient of a secreted morphogen (15, 16), or by physically stimulating sensory monocilia on cells in the periphery of the node (17). Consistent with the pivotal role of these monocilia in left–right determination, mutations that affect the formation (15, 18–24), sensory function (25), or motility (26, 27) of monocilia in the node region disrupt the normal generation of left–right asymmetry.

Information on the regulation of expression of proteins essential for cilia formation and function in the node region is still scarce: *Rfx3* and *Foxj1*, members of the RFX and forkhead family of transcription factors, respectively, are expressed in the node and in many tissues containing ciliated cells (28, 29). Loss of RFX3 leads to short but ultrastructural apparently normal cilia, left–right defects, and reduced expression of *D2lic*, a cytoplasmic dynein implicated in intraflagellar transport (30). Loss of FOXJ1 causes absence of cilia and loss of left–right dynein (*Dnahc11*) expression in lung epithelial cells, and, in addition, left–right defects (29, 31), although apparently normal cilia were observed in the node region (29). Thus, it appears that, in the node region, the components important for ciliogenesis and cilia function are differently regulated. Here, we show that loss of *Noto* function in $Noto^{GFP}$ mice disrupts the formation and function of the PNC and cilia, and consequently the establishment of normal left–right asymmetry. Our results establish *Noto* as a key regulator of ciliogenesis in the mouse PNC upstream of *Foxj1* and *Rfx3*.

## Results

**Defective Left–Right Determination in *Noto* Mutants.** Embryos homozygous for the null $Noto^{GFP}$ allele showed defects in the caudal notochord and occasionally also at more anterior levels, and most mutants died shortly after birth (7). Urogenital or anorectal malformations that can be associated with defective notochord development (32, 33) were not observed in homozygous $Noto^{GFP}$ newborns (7). Detailed inspection of the visceral organs now revealed laterality defects in a large fraction of mutants (Fig. 1 *A–F* and data not shown). E16.5 $Noto^{GFP/GFP}$ embryos displayed heterotaxia ($n = 2$ of 32), left ($n = 11$ of 32; Fig. 1*D*) and right ($n = 4$ of 32; Fig. 1*E*) isomerism of the lung,

Author contributions: A.G. designed research; A.B., L.A., and C.V. performed research; P.A. contributed new reagents/analytic tools; A.B., L.A., C.V., and A.G. analyzed data; and A.G. wrote the paper.

The authors declare no conflict of interest.

This article is a PNAS Direct Submission.

Abbreviations: E(*n*), embryonic day *n*; PNC, posterior notochord.

§To whom correspondence should be addressed. E-mail: gossler.achim@mh-hannover.de.

This article contains supporting information online at www.pnas.org/cgi/content/full/0704344104/DC1.

© 2007 by The National Academy of Sciences of the USA

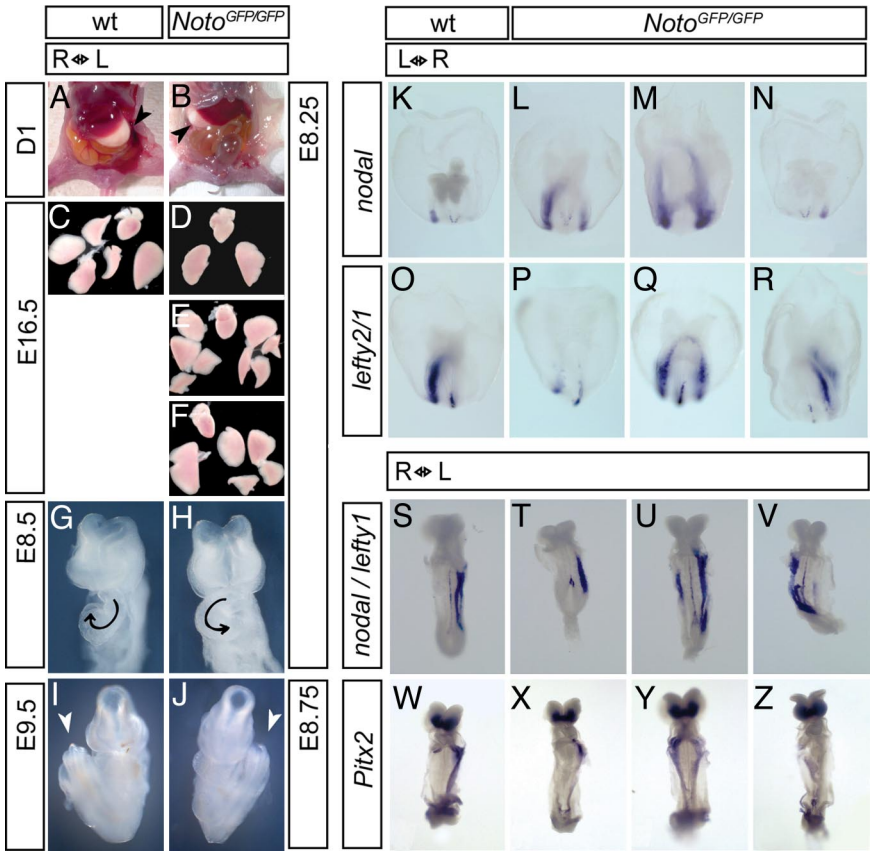


**Fig. 1.** Laterality defects in *Noto*$^{GFP}$ mutants (*A–F*) Situs of visceral organs in wild-type (*A* and *C*) and mutant (*B* and *D–F*) newborns (*A* and *B*) and E16.5 embryos (*C–F*). Heart looping (*G* and *H*) and embryonic turning (*I* and *J*) in wild-type (*G* and *I*) and mutant (*H* and *J*) embryos are shown. Age of the embryos is indicated to the left. (*K–Z*) Whole-mount *in situ* hybridization of wild-type and three different representative mutant embryos with probes (indicated to the left) for asymmetrically expressed genes. R ↔ L indicates the orientation of the embryos. Genotypes are indicated at the top.

complete *situs inversus* ($n$ = 9 of 32; Fig. 1*F*) and *situs solitus* ($n$ = 6 of 32). Consistent with laterality defects, a significant portion of mutant fetuses at E18.5 showed obvious macroscopic abnormalities in the outflow tracts [supporting information (SI) Fig. 5] providing a plausible explanation for the high postnatal mortality reported previously (7).

Consistent with the abnormal *situs* of visceral organs, heart looping (Fig. 1 *G* and *H*) and embryonic turning (Fig. 1 *I* and *J*), and the expression patterns of asymmetrically expressed genes were randomized (Fig. 1 *K–Z*). *Nodal*, which is expressed in the left lateral plate mesoderm (lpm) in wild-type E8.25 (3–6 somites) embryos was expressed normally (2 of 10), bilaterally (4 of 10), or in the right lpm (1 of 10), or expression was severely reduced in the lpm (3 of 10) of homozygous *Noto*$^{GFP}$ embryos (Fig. 1 *K–N* and *S–V* and data not shown). *Lefty2* expression was similarly affected, mutant embryos showing normal left-sided (2 of 8), bilateral (2 of 8), right-sided (3 of 8), or severely down-regulated (1 of 8) expression (Fig. 1 *O–V* and data not shown). *Lefty1* expression in the midline was present in the majority of the analyzed embryos (6 of 8), although at variable levels, and, in some cases, the contiguous expression domain was interrupted (data not shown). Also, expression of *Pitx2*, which acts downstream of *nodal* (34), was randomized in E8.75 mutants (7–10 somites), with normal left-sided (1 of 7), bilateral (4 of 7), right sided (1 of 7), and no expression (1 of 7; Fig. 1 *W–Z* and data not shown). Given the importance of the organizer for patterning the anterior–posterior neuraxis (35–38) and *Noto* expression in the organizer (6), we analyzed anterior–posterior patterning in *Noto* E8.75 null mutant embryos. The expression patterns of *Fgf8*, *Gbx2*, *Krox20*, and *Otx2* were indistinguishable in wild-type and *Noto* mutants (data not shown), suggesting that anterior–posterior patterning occurs normally. Collectively, these results indicated that *Noto* is essential for establishing left–right asymmetry and suggested that *Noto* function is required in the node before or during establishment of asymmetric gene expression.

**Disrupted Node Structure in *Noto* Mutants.** In wild-type embryos at E8.0, the peripheral "crown cells" (39) of the node region express *nodal* and *dante*, with stronger expression on the left or right side, respectively (Fig. 2 *A*, *E*, *I*, and *M*; see also refs. 40 and 41). At this stage, *Noto* expression was detected in the central cells of the PNC [also called "pit cells" (39)] and appeared largely nonoverlapping with these expression domains (Fig. 2*Q*). This interpretation was supported by double *in situ* hybridizations that showed that *Noto* and *dante* are coexpressed only in a subset of peripheral cells (arrowheads in Fig. 2*R*). In the majority of mutant embryos, expression domains of *nodal* and *dante* were irregular and variable, or consisted of scattered groups of cells only in the PNC region (Fig. 2 *B–D*, *F–H*, *J–L*, and *N–P* and data not shown), and *dante*-expressing cells were intermingled with cells expressing *gfp* from the *Noto* locus (Fig. 2 *S–U*), suggesting that typical PNC (or pit) cells and crown cells are present, but the node is disorganized. Consistently, by scanning electron microscopy, a distinct node was hardly detected in 12 of 21 E7.5–E8.0 mutant embryos, whereas the remainder had small and irregular nodes with no sharp border between pit and crown cells (Fig. 3 *Ae*, *Af*, *Ai*, and *Aj*), or with pit cells separated into noncoherent groups (red circles in Fig. 3*Aj*).

**Abnormal Cilia Structure in *Noto* Mutants.** Mutant PNC cells had monocilia and microvilli, although the number of cilia-bearing

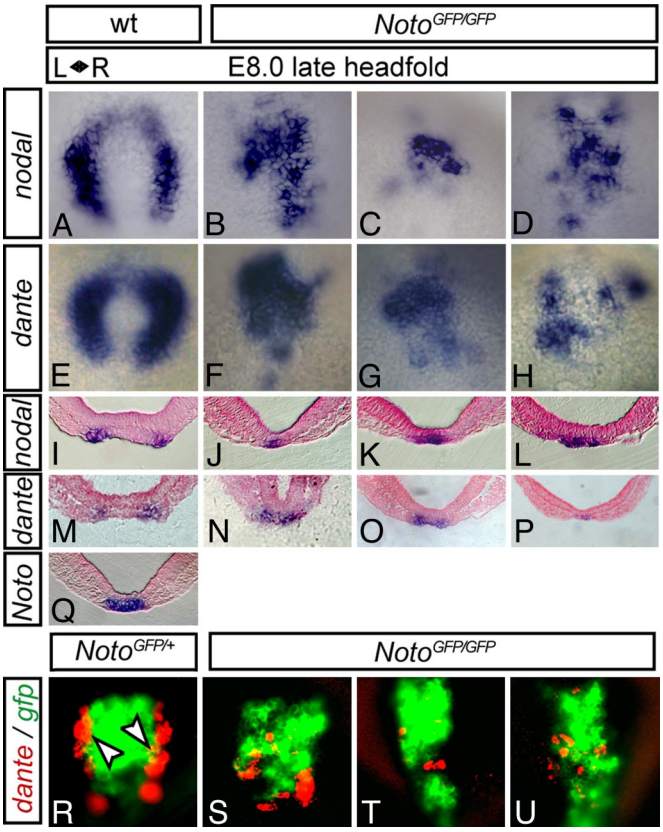


**Fig. 2.** Node/PNC defects in *Noto*$^{GFP}$ mutants. (*A–H*) Pictures of the node after whole-mount *in situ* hybridization with probes for *nodal* (*A–D*) and *dante* (*E–H*). (*I–Q*) Eosin-counterstained sections of plastic-embedded embryos after whole-mount *in situ* hybridization. (*R–U*) False-color double (fluorescent–colorimetric) whole-mount *in situ* hybridization with *dante* (red) and *gfp* (green; false color). The arrowheads in *R* point to cells with overlapping *dante* and *gfp* expression. L ↔ R indicates the orientation of the embryos. Genotypes are indicated at the top.

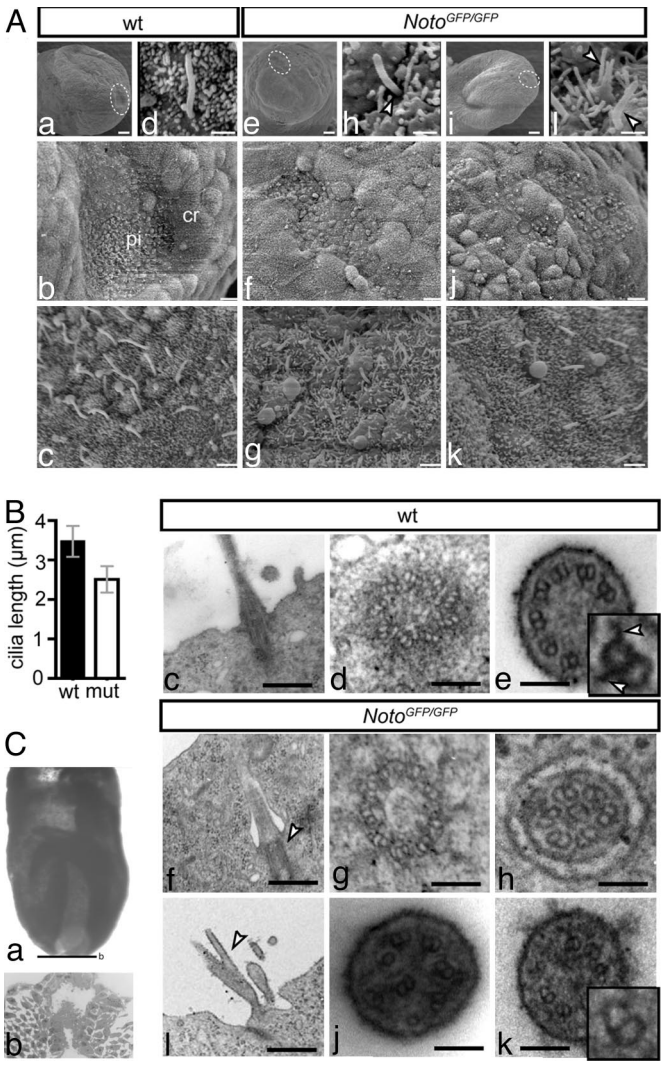


**Fig. 3.** Abnormal node/PNC and cilia structure in *Noto*$^{GFP}$ mutants. (*A*) Scanning electron micrographs of E7.5 wild-type (*Aa–Ad*) and mutant (*Ae–Al*) embryos. Dotted circles in *Aa*, *Ae*, and *Ai*) indicate the node region. Red circles in *Aj* point to noncoherent groups of pit cells. Arrowhead in (*Ah*) points to a cilium emerging from an indentation of the plasma membrane. Arrowheads in *Al* point to bundled and elongated microvilli and to a shortened cilium, respectively. (*B*) Reduction of cilia length in mutant embryos ($P < 0.0001$) compared with wild-type. Error bars indicate standard deviation. (*C*) Transmission electron micrographs of E7.5 wild-type (*Cc–Ce*) and mutant (*Cf–Ck*) embryos. In *Ca* and *Cb*, the plane of sectioning is shown. *Cc* and *Cf* show saggital sections through a cilium and the corresponding basal body. The arrowhead in *Cf* points to an abnormally located basal body. The microvilli shown in *Ci* are elongated and branched (arrowhead). The structure of basal bodies in transverse sections *Cd* and *Cg* appeared normal. Transverse sections of mutant cilia (*Ch*, *Cj*, and *Ck*) show variably arranged microtubuli with or without a central microtubular structure instead of the normal wild-type (*Ce*) arrangement of 9 + 0 tubuli. Arrowheads in *Ce* point to inner and outer dynein arms that are frequently missing in mutant cilia *Ck*. The cilium in *Ch* emerges from an abnormally located basal body. (Scale bars in *A* represent 1 μm in *Ad*, *Ah*, and *Al*; 2 μm in *Ac*, *Ag*, and *Ak*; 10 μm in *Ab*, *Af*, and *Aj*; and 50 μm in *Aa*, *Ae*, and *Ai*; scale bars in *C* represent 300 nm in *Cc*, *Cf*, and *Ci* and 100 nm in *Cd*, *Ce*, *Cg*, *Ch*, *Cj*, and *Ck*).

cells appeared reduced (Fig. 3 *Ac*, *Ag*, and *Ak*), and cilia were significantly shorter (Fig. 3*B*). Some cilia emerged from indentations of the plasma membrane (Fig. 3*Ah*), and microvilli were bundled and variable in length (Fig. 3*Al*), suggesting that the structure of cilia and microvilli is abnormal. Transmission electron microscopy of mutant embryos ($n = 11$) showed that some microvilli were branched (Fig. 3*Ci*), and mutant cilia contained a variable number (3–8, rarely 9) of partly disorganized or incomplete, irregularly arranged peripheral microtubular doublets with or without a central microtubule (Fig. 3 *Ch*, *Cj*, and *Ck*). In addition, dynein arms were frequently missing (*Insets* in Fig. 3*Ck*). Consistent with abnormal cilia structure, the majority of cilia were immotile in seven analyzed mutant embryos (SI Movies 1–3). The structure of the basal bodies appeared normal (Fig. 3*Cg*). However, of 41 basal bodies found in ultrathin sections, only 10 were located in the cortex, whereas 14 were obviously located abnormally deep in the cytoplasm (Fig. 3*Cf* and data not shown), and the location of the remainder could not unambiguously be determined in the available sections. Taken together, abnormal morphology in the node region and aberrant cilia structure in mutants indicate a role(s) for *Noto* in the regulation of PNC formation, ciliogenesis, and the establishment of left–right asymmetry.

**Altered Expression of Genes Implicated in Ciliogenesis or Function.** In line with the abnormal location of basal bodies in *Noto* mutant PNC cells and defective basal body anchoring in lung epithelium cells in *Foxj1* mutants (29, 42) *Foxj1* transcripts were barely detectable in mutant node regions (Fig. 4 *A–C*), indicating that *Noto* acts upstream of *Foxj1*. Expression of the axonemal dynein *Dnahc11*, which is regulated by *Foxj1* in lung epithelial cells (31) and required for cilia motility, was down-regulated (Fig. 4 *D–F*) and *Dnahc5*, an axonemal dynein that is expressed in the node

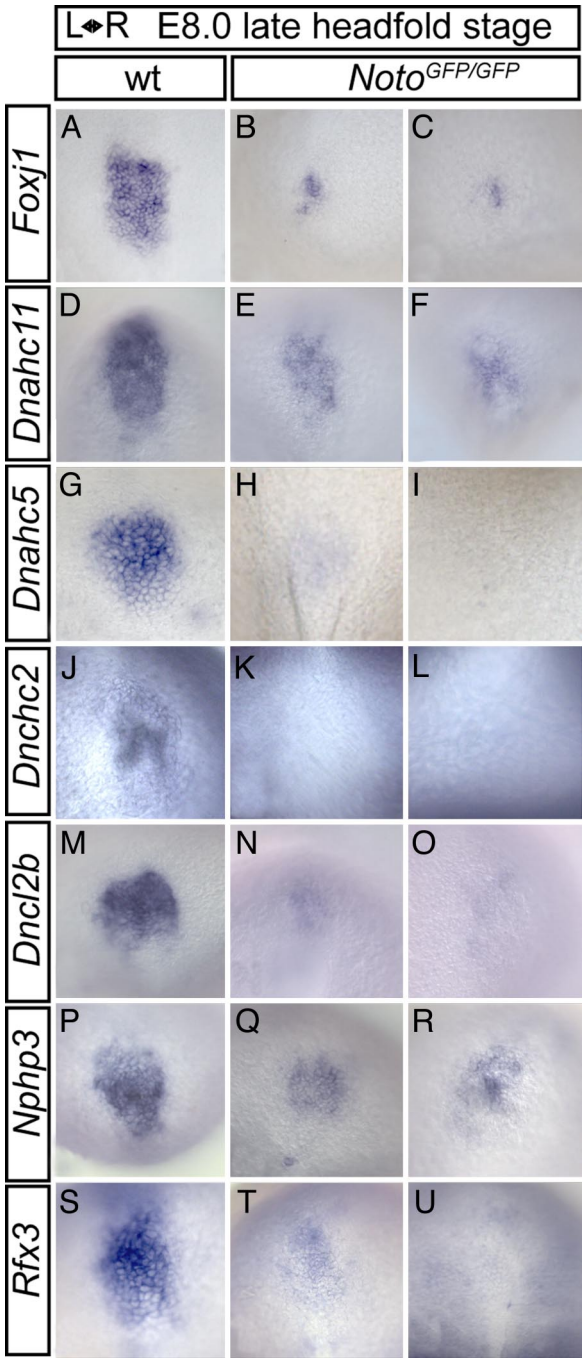


**Fig. 4.** Expression of potential *Noto* target genes. Whole-mount *in situ* hybridization of E8.0 wild-type and mutant embryos. Genotypes are indicated at the top, used probes are indicated on the left. Pictures are taken from the node region.

and required for the formation of outer dynein arms (43), and *Dnchc2*, a component of retrograde intraflagellar transport required for normal cilia morphology (21, 44), were not detected in mutant nodes (Fig. 4 *G–L*). In addition, expression of the cytoplasmic dynein *Dncl2b* in mutant nodes was essentially abolished (Fig. 4 *M–O*). Transcripts of *Nphp3*, encoding a protein that might be involved in microtubule organization and is mutated in Nephronophtisis3 patients and normally expressed in the node region (45), were significantly down-regulated in mutant embryos (Fig. 4 *P–R*). Finally, *Rfx3*, which is required for normal cilia growth (30), was severely down-regulated in the node regions of *Noto* mutant embryos (Fig. 4 *S–U*). Collectively, these results establish *Noto* as a transcription factor upstream of *Foxj1* and *Rfx3* that is essential for the expression of multiple proteins required for cilia formation and function.

## Discussion

We show that the homeobox gene *Noto* is essential for cilia formation in the PNC and for left–right patterning. *Noto* acts upstream of *Foxj1* and *Rfx3* in this process and is required for the expression of various components important for axonemal assembly and function. In addition, *Noto* is required for PNC morphogenesis but seems to be dispensable for anterior–posterior patterning functions of the organizer.

**A Conserved Function of *Noto* in Formation of "Organs of Asymmetry".** The majority of *Noto* mutants showed variable defects in the PNC that ranged from complete absence over variable size and shape and disorganized distribution of crown and pit cells to apparently normal morphology in rare cases. These findings indicate a major function of *Noto* in node and posterior notochord morphogenesis and suggest an essential role in regulating migration, positioning, or separation of crown and pit cells. Because *Noto* is expressed in the pit cells, but only some crown cells, *Noto* function might predominantly be required in pit cells. Abnormal migration and positioning of notochord precursors might also underlie defective notochord development in *Noto* mutants at later stages. This aspect of *Noto* function appears to be conserved among mammals, amphibia, and teleost fish. In teleosts, a transient spherical ciliated structure called Kupffer's vesicle functions in the establishment of left–right asymmetry equivalent to the amphibian gastrocoel roof plate and the mammalian PNC (12, 13, 46, 47). In zebrafish embryos mutant for the *Noto* homologue *flh*, Kupffer's vesicles were abnormally small and irregularly shaped (48). Kupffer's vesicle is formed from a distinct population of cells that migrate at the leading edge of the embryonic shield (49), the zebrafish equivalent of the organizer (50). Similarly, the precursors of the mouse node and notochord represent a distinct cell population that resides posterior to the midgastrulation organizer in midstreak-stage mouse embryos (51). Thus, it appears that, in mammals and teleost fish, *Noto*/*flh* regulates aspects of cell behaviour in a group of cells that is associated with the organizer and fated to form a functionally analogous specialized structure required for left–right patterning. Asymmetry defects have been described in *flh* mutants but were attributed to the complete absence of the notochord (52). Our data and abnormal Kupffer's vesicles observed by Melby *et al.* (48) in *flh* mutants both support the view that abnormal Kupffer's vesicle formation contributes to the left–right patterning defects in *flh* mutants.

***Noto* as Regulator Of Nodal Ciliogenesis Upstream of *Foxj1* and *Rfx3*.** A striking feature of the *Noto* phenotype is the highly variable abnormal structure of cilia. These abnormalities likely arise from the reduced or missing expression of genes encoding proteins that are essential for cilia motility or axonemal assembly or transport. Because mutations that affect single components required for the formation (15, 18–24), sensory function (25), or motility (26, 27) of nodal monocilia, respectively, disrupt the normal generation of left–right asymmetry, cilia in *Noto* mutants are most likely nonfunctional. Our results suggest that *Noto* is pivotal for the coordinate expression of essential components of the functional axonemal complex in the mouse PNC. However, the role of Not homeobox genes in regulating ciliogenesis in amphibian and fish embryos is currently not clear, whereas it appears irrelevant in avian embryos, where cells in the notochord region equivalent to teleost Kupffer's vesicle, the amphibian gastrocoel roof plate, and the mammalian PNC do not exhibit monocilia (53) despite expression of *Gnot1* and *Gnot2* (54–56).

It is unlikely that *Noto* acts as a direct regulator of all

deregulated axonemal genes. Down-regulation of *Foxj1* and *Dnahc11*, which is regulated by *Foxj1* in respiratory epithelial cells (31), suggests that *Foxj1* acts as a mediator of *Noto* function in the node. This notion is further supported by the abnormal position of basal bodies in node cells, which closely resembles the phenotype in lung epithelial cells in *Foxj1* mutants (42). The severe reduction of *Foxj1* indicates that *Foxj1* acts downstream of *Noto*, although residual *Foxj1* expression suggests that other factor(s) also activate *Foxj1*. In contrast, *Rfx3* expression was virtually abolished in the node regions of mutant embryos, which might indicate that *Noto* is the major activator of *Rfx3* expression in the node region. In conclusion, our results suggest a general requirement of *Noto* for assembly and function of cilia in vertebrate organs of asymmetry.

## Methods

**Mice.** $Noto^{GFP/GFP}$ mice were genotyped as described (7).

**Histology and Scanning Electron Microscopy.** After whole-mount *in situ* hybridization, embryos were embedded in HISTORESIN embedding medium (Leica, Wetzlar, Germany). Sections were cut at 2 $\mu$m, counterstained with eosin, and analyzed with a DM5000B microscope, a DFC300FX camera, and FireCam software (Leica). For scanning electron microscopy, dissected embryos were immersion-fixed in 3% glutaraldehyde–0.1M cacodylate buffer (pH 7.4) at 4°C overnight, washed in 0.1 M cacodylate buffer (four times for 10 min each), postfixed in 2% osmium tetroxide in 0.1 M cacodylate buffer at room temperature in the dark, dehydrated in a graded acetone series, critical point dried, mounted and sputter coated with gold, and viewed under a SEM 505 microscope (Philips, Eindhoven, The Netherlands).

***In Situ* Hybridization.** Mutant and wild-type embryos were processed in parallel under identical conditions by standard procedures. Double *in situ* hybridization was done by simultaneous hybridization of a Digoxigenin-labeled *dante* and fluorescein-labeled *gfp* probe. Bound probes were detected by using HRP-coupled anti-DIG antibodies and Cy3 tyramid signal amplification (TSA PlusFluorescence System; PerkinElmer, Waltham, MA), followed by BM-purple staining using AP-conjugated anti-fluorescein antibodies. Images were obtained with a DM5000B microscope, a DFC300FX camera, and FireCam software (Leica) or a M420 microscope (Leica) and HC300Z camera (Fuji, Tokyo, Japan) and FujixPhotograb300Z software (Fuji). Images were processed by using Photoshop CS (Adobe, San Jose, CA). False color images were generated by inserting an inverted bright-field image of the BM purple staining into the green channel of the Cy3 image and adjustments of the green and red channel, respectively.

**Transmission Electron Microscopy.** Standard procedures were applied for fixation (1.5% glutaraldehye and 1.5% paraformaldehyde in phosphate buffer) of mutant and wild-type embryos. Thin sectioning of selected serial semithin sections (57) enabled faithful localization and transmission electron microscopy of cilia and their related structures.

**Cilia Measurements.** One hundred nine and 93 cilia from four wild-type and mutant embryos, respectively, were measured in scanning electronmicrographs by using the ImageJ software (National Institutes of Health, Bethesda, MD, http://rsb.info.nih.gov/ij/). Statistical analysis was done by using an unpaired *t* test with the Prism software (GraphPad, San Diego, CA).

**Measurement of Cilia Motility.** Motility of cilia was analyzed by videomicroscopy essentially as described (13).

We thank José António Belo (Instituto Gulbenkian de Ciência, Oeiras, Portugal), Martin Blum (University of Hohenheim, Stuttgart, Germany), Martina Brückner (Yale University School of Medicine, New Haven, CT), Bénédicte Durand (Université Claude Bernard, Villeurbanne, France), Brian P. Hackett (Washington University School of Medicine, St. Louis, MO), Andreas Kispert (Medizinische Hochschule, Hannover, Germany), and Janet Rossant (Hospital for Sick Children Research Institute, Toronto, ON, Canada) for probes; Stephanie Groos and Gerhard Preiss for help with the scanning electron microscopy; Thomas Grieskamp for help with outflow tract analysis; Kerstin Brekerbohm and Peter Schwartz for help with the transmission electron microscopy; and Anne Camus and Jérome Collignon for teaching fluorescent *in situ* hybridization to A.B. This work was supported by a German Research Council grant (to A.G.).

1. Tam PPL, Gadd JM (2004) in *Gastrulation: From Cells to Embryo*, ed Stern C (Cold Spring Harbor Lab Press, Cold Spring Harbor, NY), pp 233–262.
2. De Robertis EM (2006) *Nat Rev Mol Cell Biol* 7:296–302.
3. Camus A, Tam PP (1999) *Curr Top Dev Biol* 45:117–153.
4. Viebahn C (2001) *Genesis* 29:96–103.
5. Mackem S (2004) in *Gastrulation: From Cells to Embryo*, ed Stern CD (Cold Spring Harbor Lab Press, Cold Spring Harbor, NY), pp 599–607.
6. Plouhinec JL, Granier C, Le Mentec C, Lawson KA, Saberan-Djoneidi D, Aghion J, Shi DL, Collignon J, Mazan S (2004) *Gene Expr Patterns* 5:11–22.
7. Abdelkhalek HB, Beckers A, Schuster-Gossler K, Pavlova MN, Burkhardt H, Lickert H, Rossant J, Reinhardt R, Schalkwyk LC, Muller I, *et al.* (2004) *Genes Dev* 18:1725–1736.
8. Blum M, Andre P, Muders K, Schweickert A, Fischer A, Bitzer E, Bogusch S, Beyer T, van Straaten HW, Viebahn C (2007) *Differentiation* 75:133–146.
9. Sulik K, Dehart DB, Inagaki T, Carson JL, Vrablic T, Gesteland K, Schoenwolf GC (1994) *Dev Dyn* 201:260–278.
10. Satir P, Christensen ST (2007) *Annu Rev Physiol* 69:377–400.
11. Feistel K, Blum M (2006) *Dev Dyn* 235:3348–3358.
12. Kramer-Zucker AG, Olale F, Haycraft CJ, Yoder BK, Schier AF, Drummond IA (2005) *Development (Cambridge, UK)* 132:1907–1921.
13. Schweickert A, Weber T, Beyer T, Vick P, Bogusch S, Feistel K, Blum M (2007) *Curr Biol* 17:60–66.
14. Nonaka S, Shiratori H, Saijoh Y, Hamada H (2002) *Nature* 418:96–99.
15. Nonaka S, Tanaka Y, Okada Y, Takeda S, Harada A, Kanai Y, Kido M, Hirokawa N (1998) *Cell* 95:829–837.
16. Okada Y, Takeda S, Tanaka Y, Belmonte JC, Hirokawa N (2005) *Cell* 121:633–644.
17. McGrath J, Somlo S, Makova S, Tian X, Brueckner M (2003) *Cell* 114:61–73.
18. Marszalek JR, Ruiz-Lozano P, Roberts E, Chien KR, Goldstein LS (1999) *Proc Natl Acad Sci USA* 96:5043–5048.
19. Taulman PD, Haycraft CJ, Balkovetz DF, Yoder BK (2001) *Mol Biol Cell* 12:589–599.
20. Houde C, Dickinson RJ, Houtzager VM, Cullum R, Montpetit R, Metzler M, Simpson EM, Roy S, Hayden MR, Hoodless PA, *et al.* (2006) *Dev Biol* 300:523–533.
21. Huangfu D, Anderson KV (2005) *Proc Natl Acad Sci USA* 102:11325–11330.
22. Huangfu D, Liu A, Rakeman AS, Murcia NS, Niswander L, Anderson KV (2003) *Nature* 426:83–87.
23. Murcia NS, Richards WG, Yoder BK, Mucenski ML, Dunlap JR, Woychik RP (2000) *Development (Cambridge, UK)* 127:2347–2355.
24. Takeda S, Yonekawa Y, Tanaka Y, Okada Y, Nonaka S, Hirokawa N (1999) *J Cell Biol* 145:825–836.
25. Pennekamp P, Karcher C, Fischer A, Schweickert A, Skryabin B, Horst J, Blum M, Dworniczak B (2002) *Curr Biol* 12:938–943.
26. Watanabe D, Saijoh Y, Nonaka S, Sasaki G, Ikawa Y, Yokoyama T, Hamada H (2003) *Development (Cambridge, UK)* 130:1725–1734.
27. Supp DM, Witte DP, Potter SS, Brueckner M (1997) *Nature* 389:963–966.
28. Reith W, Ucla C, Barras E, Gaud A, Durand B, Herrero-Sanchez C, Kobr M, Mach B (1994) *Mol Cell Biol* 14:1230–1244.
29. Brody SL, Yan XH, Wuerffel MK, Song SK, Shapiro SD (2000) *Am J Respir Cell Mol Biol* 23:45–51.
30. Bonnafe E, Touka, M., AitLounis A, Baas D, Barras E, Ucla C, Moreau A, Flamant F, Dubruille R, Couble P, *et al.* (2004) *Mol Cell Biol* 24, 4417–4427.
31. Chen J, Knowles HJ, Hebert JL, Hackett BP (1998) *J Clin Invest* 102:1077–1082.
32. Berry RJ (1960) *Genet Res* 1:439–451.
33. Gluecksohn-Schoenheimer S (1943) *Genetics* 28:341–348.

34. Lin CR, Kioussi C, O'Connell S, Briata P, Szeto D, Liu F, Izpisúa-Belmonte JC, Rosenfeld MG (1999) *Nature* 401:279–282.
35. Ang SL, Conlon RA, Jin O, Rossant J (1994) *Development (Cambridge, UK)* 120:2979–2989.
36. Ang S-L, Behringer RR (2002) in *Mouse Development*, eds Rossant J, Tam PPL (Academic, San Diego), pp 37–53.
37. Klingensmith J, Ang S-L, Bachiller D, Rossant J (1999) *Dev Biol* 216:535–549.
38. Tam PPL, Steiner KA (1999) *Development (Cambridge, UK)* 126:5171–5179.
39. Bellomo D, Lander A, Harragan I, Brown NA (1996) *Dev Dyn* 205:471–485.
40. Marques S, Borges AC, Silva AC, Freitas S, Cordenonsi M, Belo JA (2004) *Genes Dev* 18:2342–2347.
41. Conlon FL, Lyons KM, Takaesu N, Barth KS, Kispert A, Herrmann B, Robertson EJ (1994) *Development (Cambridge, UK)* 120:1919–1928.
42. Gomperts BN, Gong-Cooper X, Hackett BP (2004) *J Cell Sci* 117:1329–1337.
43. Olbrich H, Haffner K, Kispert A, Volkel A, Volz A, Sasmaz G, Reinhardt R, Hennig S, Lehrach H, Konietzko N, *et al.* (2002) *Nat Genet* 30:143–144.
44. May SR, Ashique AM, Karlen M, Wang B, Shen Y, Zarbalis K, Reiter J, Ericson J, Peterson AS (2005) *Dev Biol* 287:378–389.
45. Olbrich H, Fliegauf M, Hoefele J, Kispert A, Otto E, Volz A, Wolf MT, Sasmaz G, Trauer U, Reinhardt R, *et al.* (2003) *Nat Genet* 34:455–459.
46. Essner JJ, Amack JD, Nyholm MK, Harris EB, Yost HJ (2005) *Development (Cambridge, UK)* 132:1247–1260.
47. Essner JJ, Vogan KJ, Wagner MK, Tabin CJ, Yost HJ, Brueckner M (2002) *Nature* 418:37–38.
48. Melby AE, Warga RM, Kimmel CB (1996) *Development (Cambridge, UK)* 122:2225–2237.
49. Cooper MS, D'Amico LA (1996) *Dev Biol* 180:184–198.
50. Shih J, Fraser SE (1996) *Development (Cambridge, UK)* 122:1313–1322.
51. Kinder SJ, Tsang TE, Wakamiya M, Sasaki H, Behringer RR, Nagy A, Tam PP (2001) *Development (Cambridge, UK)* 128:3623–3634.
52. Danos MC, Yost HJ (1996) *Dev Biol* 177:96–103.
53. Manner J (2001) *Anat Embryol (Berlin)* 203:481–490.
54. Knezevic V, Ranson M, Mackem S (1995) *Dev Biol* 171:458–470.
55. Stein S, Kessel M (1995) *Mech Dev* 49:37–48.
56. Stein S, Niss K, Kessel M (1996) *Dev Biol* 180:519–533.
57. Miething A (1992) *Microsc Res Tech* 21:73–74.